JOURNAL OF SOLID STATE CHEMISTRY **133,** 516–521 (1997)
ARTICLE NO. SC977520

$Pb_2BiO_2PO_4$, a New Oxyphosphate

Ariane Mizrahi,*,[1] Jean-Pierre Wignacourt,* and Hugo Steinfink†

* *Laboratoire de Cristallochimie et Physicochimie du Solide, ENSCL, BP 108, 59652 Villeneuve d'Ascq Cedex, France; and*
† *Department of Chemical Engineering, University of Texas, Austin, Texas 78712*

Received February 21, 1997; in revised form June 16, 1997; accepted June 23, 1997

$Pb_2BiO_2PO_4$ is orthorhombic with space group *Pnma*, $a = 5.930(4)$, $b = 9.079(10)$, $c = 11.473$ (6) Å at room temperature, $Z = 4$, and a congruent melting point of 860°C. The structure was solved from single crystal and powder diffraction data. The PO_4 ion can occupy two energetically equivalent positions causing two oxygen atoms to be disordered. The structure can be described on the basis of several motifs. Infinite chains of BiO_2 rectangular pyramids formed by edge-sharing parallel to the *a* axis that are linked by lead atoms and phosphate anions. Bi can also be considered as present in a trigonal prismatic environment of oxygen atoms in which one corner of a triangular face is unoccupied. Presumably the $6s^2$ lone pair extends toward that apex. Pb is bonded to six oxygen atoms forming a distorted octahedron when distances less than 3 Å are considered. When two additional oxygen ions at 3.20(9) and 3.24(5) Å are considered part of the coordination polyhedron it can be described as a bisdisphenoid. This structure is related to structures found in many $M_2^{II}BiXO_6$ phases. The Raman spectrum shows the expected frequencies for PO_4. In addition frequencies are observed that can be assigned to P–O–Bi and P–O–Pb linkages. Intense bands at 143 and 150 cm^{-1} are attributed to internal vibrational modes of the BiO_4 pyramid.

INTRODUCTION

Interest in compounds with the stoichiometry $Pb_2M^{III}XO_6$ exists because they display magnetic, electro-optic, anion transport, and laser properties. The compounds Pb_2FeNbO_6 and Pb_2NiNbO_6 have the perovskite structure (1), while Pb_2SbNbO_6 (2) and Pb_2BiTaO_6 (3) crystallize in the pyrochlore structure. Another structure type has been observed for recently synthesized compounds in which the trivalent cation is Bi^{3+}. The compounds Mg_2BiXO_6, $X = V$ (4), P, As (5), Cu_2BiPO_6 (6), and Cd_2BiPO_6 (7) have very similar crystal structures. The main differences exist among the coordination polyhedra around the divalent cations. The structures of Cu_2BiVO_6 and Zn_2BiPO_6 are not known but they have lattice parameters similar to the other members of this family. In particular the system Bi_2O_3–PbO was extensively investigated (8) and the discovery of oxide ion conductivity in $Bi_4V_2O_{11}$ (9) stimulated further research on the pseudo-ternary system Bi_2O_3–V_2O_5–M_xO_y (10). The crystal structures of the Bi^{3+} phases display anisotropic electronic properties because of the presence of the nonbonding $6s^2$ lone pair of electrons. Similar characteristics are displayed by Pb^{2+} containing compounds. For this reason we investigated the Bi_2O_3–V_2O_5–PbO system and identified the compound Pb_2BiVO_6 among others (11). It has four allotropic forms and their X-ray powder diffraction patterns are complex. We hoped that the substitution of P for V would simplify the crystal chemical behavior and we report here the structural investigation of Pb_2BiPO_6.

EXPERIMENTAL

The powder sample was prepared by solid-state reaction between the required proportions of $(NH_4)_2HPO_4$ (Fluka Chemika, purity >99%), PbO (Aldrich, purity >99.9%), and Bi_2O_3 (Riedel–de Haën, purity >99.9%). Prior to using the oxides they were heated at 600°C to remove any carbonates. A stoichiometric mixture of the reactants was placed in a gold container and heated initially at 280°C to remove any moisture; the temperature was then raised to 570°C to decompose the ammonium phosphate. The reaction was complete after annealing at 700°C for 4 days with intermediate grinding. The progress of the reaction was checked using X-ray diffraction analysis with a Guinier-de Wolff camera and Cu$K\alpha$ radiation. The final pattern of the compound was recorded between 10° and 75° 2θ on a D5000 Siemens diffractometer equipped with a diffracted-beam graphite monochromator and Cu$K\alpha$ radiation. The diffraction angle positions were refined using a profile fitting program and the pattern was indexed with the use of the program TREOR (12). Lattice parameters were obtained from a least-squares procedure. Density measurements were performed with an automated Micromeritics Accupyc 1330 gas pycnometer equipped with a 1 cm^3 cell.

A small amount of powdered Pb_2BiPO_6 was placed in a gold container. The temperature was ramped to 870°C at

[1] To whom correspondence is to be addressed.

0022-4596/97 $25.00

100°C h^{-1}, held at 870°C for 12 h, cooled to 670°C at 2°C h^{-1}, followed by cooling to 460°C at 5°C h^{-1}, and then furnace cooled to room temperature. At the end of this procedure the crucible contained irregular yellow crystals. Several crystals were selected and investigated on an automated single-crystal diffractometer as well as by Weissenberg methods. The data for the Rietveld refinement were recorded on a D5000 Siemens diffractometer between 10° and 120° 2θ in steps of 0.025° with a count time of 40 s. The FULLPROF program was used for the refinement (13).

Differential thermal analysis (DTA) was performed on a Du Pont 1090B thermal analyzer using a 1600 differential thermal analysis cell (heating rate 5°C min^{-1}). The possibility of phase changes was investigated with a high-temperature X-ray diffraction (HTXRD) Guinier–Lenné camera at a heating rate of 20°C h^{-1}.

Raman spectra were recorded with a RTI DILOR spectrometer; spectral resolution was 0.5–1 cm^{-1}, power 25 mW; exiting radiation was 647.1 nm from a Kr^+ laser.

RESULTS

Using the 20 most intense reflections of the X-ray diffraction powder pattern, the indexing program TREOR (12) yielded orthorhombic lattice parameters. All observed reflections were indexed and the figures of merit were $F_{20} = 14$ and $M_{20} = 17$. After a least-squares refinement, the cell parameters were $a = 5.935(1)$, $b = 9.101(2)$, and $c = 11.496(2)$ Å. The indexed powder diffraction pattern is shown in Table 1. The calculated density, $d_{calc.} = 8.07$ g cm^{-3}, is in good agreement with that measured, $d_{meas.} = 7.93$ g cm^{-3}, yielding four formula weights per unit cell. A DTA curve exhibits a single endothermic peak at 860°C that is assigned to the melting point. The HTXRD patterns do not change with temperature confirming the DTA result that no polymorphic phase transition occurs in this compound.

Most of the crystals examined with the single-crystal diffractometer displayed complicated reciprocal lattices showing that they consisted of complex intergrowths. Only two specimens yielded the cell parameters obtained from the powder sample. After many trials oscillation and Weissenberg photographs of one of the irregularly shaped crystals showed systematic absences consistent with space group *Amma*, *Cmcm* in conventional orientation. This space group is the same as that for Mg_2BiXO_6, X = V, P, As (4, 5). Three-dimensional crystallographic data and experimental parameters for the crystal structure refinement were obtained from one such irregularly shaped crystal and are shown in Table 2. Although the intense reflections agreed with the space group assignment *Amma*, there were many

TABLE 1
The Powder X-Ray Diffraction Pattern of Pb_2BiPO_6 (Cu$K\alpha$, $a = 5.935(1)$ Å, $b = 9.101(2)$ Å, $c = 11.496$ Å)

h	k	l	$d_{obs.}$	$d_{calc.}$	I/I_o (%)	h	k	l	$d_{obs.}$	$d_{calc.}$	I/I_o (%)
0	1	1	7.129	7.135	3	1	3	3	2.208	2.208	1
0	0	2	5.747	5.748	7	2	3	0	2.123	2.121	<1
0	2	0	4.560	4.550	20	1	1	5	2.086	2.087	16
1	0	2	4.126	4.129	11	2	0	4	2.065	2.065	15
1	2	2	3.059	3.058	100	0	0	6	1.916	1.916	3
1	1	3	3.034	3.035	36	3	1	1	1.907	1.907	2
2	0	0	2.996	2.968	29	2	2	4	1.879	1.880	1
0	3	1	2.934	2.933	18	3	0	2	1.871	1.871	1
0	0	4	2.874	2.874	15	2	3	3	1.855	1.856	1
2	1	1	2.740	2.740	<1	0	3	5	1.833	1.832	8
2	0	2	2.637	2.637	2	2	4	0	1.805	1.804	5
1	3	1	2.630	2.630	2	0	4	4	1.783	1.784	4
1	0	4	2.586	2.587	<1	3	2	2	1.730	1.730	13
2	2	0	2.485	2.486	1	1	5	1	1.721	1.721	4
0	2	4	2.430	2.430	1	1	2	6	1.693	1.693	4
0	3	3	2.378	2.379	3	3	3	1	1.639	1.640	1
2	0	3	2.347	2.346	<1	2	0	6	1.610	1.610	3
0	4	0	2.275	2.275	5	1	5	3	1.584	1.584	9
1	2	4	2.749	2.249	8	1	1	7	1.560	1.560	10
0	1	5	2.229	2.229	<1						

TABLE 2
Crystallographic Data and Experimental Parameters for the Crystal Structure Refinement of Pb_2BiPO_6

Color	Yellow
Crystal system	Orthorhombic
Space group	*Pnma* (62)
a (Å)	5.930(4)
b (Å)	9.079(10)
c (Å)	11.473(6)
Volume (Å^3)	617.8
Z	4
Formula weight	750.3
Calculated density g cm^{-3}	8.07
Diffractometer	CAD-4 Enraf Nonius
Radiation	Mo$K\alpha$ ($\lambda = 0.71069$ Å)
Monochromator	graphite
Temperature (°C)	23
μ (Mo) cm^{-1}	833.25
θ range (°)	2–27
Data collected	$-7 \le h \le 7$; $-11 \le k \le 11$; $-14 \le l \le 14$
Scan method	ω-2θ
No. of reflections measured	5199
No. of unique reflections with $I > 2.5\sigma(I)$	564
$R_{int.}$	0.064
Absorption corrections	ABSCOR (14)
Indices of single crystal faces, hkl, and dimensions, mm	0 1 0 0.0040; 0 1 −4 0.0030; 0 −5 −2 0.0082; 0 −1 1 0.0050; 0 2 5 0.0050; 1 1 1 0.00079; −1 −1 −3 0.00066
Transmission factors	0.03389–0.16187
Refinement method	Full-matrix least squares on $\|F\|$
Parameters varied	48
R	0.057
R_w	0.052
Goodness of fit	2.344

reflections in the three-dimensional data set that violated the space group extinction. Systematic absences were consistent with space group *Pnma*. The SHELX 76 (15) program was used for structure determination. Direct methods located the P and Bi atoms in 4*c* sites (x, 1/4, z) of *Pnma* and a peak in general position 8*d* was assigned to Pb. Another weaker peak was provisionally assigned to a second Pb atom. At this point, the refinement of the crystal structure, without the oxygen atoms, yielded $R = 0.099$. The occupancy refined to 0.75 for Pb(1). The oxygen atoms were located from electron density difference maps. O(1) and O(2) positions were determined unambiguously but two additional oxygen atoms were disordered. Their occupancies refined to 0.5. Two tetrahedral phosphate groups, $(PO_4)(1)$ and $(PO_4)(2)$, were defined with O(3) and O(6) for the first and O(4) and O(5) for the second. The final cycle of least-squares refinement with 48 parameters yielded $R = 0.057$ and $R_w = 0.052$.

Because the crystals were complexly intergrown it was not certain that the extra peaks in the Fourier maps were real or possibly due to contributions to the measured intensities from a small secondary crystal. However, a structural origin could not be ruled out. To resolve this ambiguity, a structure refinement by the Rietveld method was carried out on X-ray diffraction powder data. The heavy atom positions obtained from the single-crystal data in *Pnma* were used as initial values. Several refinement cycles clearly indicated that the peak labeled Pb(2) was spurious. It was gradually eliminated and the crystal structure contains only one crystallographically independent Pb in general position 8*d* as expected. The refinement of the oxygen atom positions was indeterminate because of their low visibility to X-rays in a structure containing such heavy metal atoms. For the final refinement 995 observations were used with 35 variable parameters yielding $\chi^2 = 3.54$, $R_P = 11.4\%$, $R_{wP} = 15.0\%$, $R_{Bragg} = 12.0\%$, and $R_F = 13.3\%$. The data from a nearly single crystal and a Rietveld X-ray diffraction powder refinement permitted the unambiguous location of Pb, Bi, and P. Some uncertainties remained concerning some of the oxygen positions that imply the existence of a phosphate anion disorder (see below). In Table 3 are listed the final atomic parameters, showing only one Pb atom but retaining the disorder for O(3)–O(4) and O(5)–O(6). Important bond distances and angles are listed in Table 4.

DISCUSSION

The space group, *Pnma*, can be related to *Cmcm*, the space group of previously mentioned Mg_2BiXO_6 phases. A similar orientation of the lattices is obtained after a permutation of the Pb_2BiPO_6 axes according to the transformation matrix (0 0 1; 1 0 0; 0 1 0). *Pnma* then becomes *Pmcn* and corresponds to *Cmcm*, except that the 2-fold axis along a is missing. This structure is closely related to the compounds M_2BiPO_6, M = Mg (5), Cu (6), Cd (7), Mg_2BiVO_6 (4), and Mg_2BiAsO_6 (5).

The crystal structure of the compound is shown in Fig. 1 in which only one of the possible two PO_4 groups is drawn. Bismuth occupies the center of a trigonal prism. One rectangular face is formed by four O(1); one O(6) is part of one triangular face but the sixth apex of the second triangular face is unoccupied. The $6s^2$ lone pair most likely extends toward that apex. Figure 2 shows one phosphate group bonded to the Bi prism through O(6). O(2) and two O(3) atoms complete the tetrahedron around P. The PO_4 disorder occurs because energetically O(4) can just as easily occupy the empty triangular site and then two O(5) atoms complete the tetrahedron. The P and O(2) atoms remain fixed in this switching process. The short P–O(6) bond, 1.41(10) Å, is unusual but considering the large value of the e.s.d. it may fall within the usual range of values (16). Such a short bond, 1.41(2) Å, is reported in P_4O_{10} (17). Bismuth

TABLE 3
Atomic Coordinates and Site Occupancies

Atom	Site	x	y	z	Occupancy	B_{eq}, Å^2
Bi	4*c*	0.2229(2) [0.2284(7)]	3/4	0.6491(1) [0.6482(3)]	1	1.76(5)
Pb	8*d*	0.2272(3) [0.2303(5)]	0.0521(2) [0.0463(2)]	0.8509(2) [0.8564(2)]	1	1.82(6)
P	4*c*	−0.257(1) [−0.261(4)]	1/4	−0.0633(7) [−0.063(1)]	1	2.32(9)
O(1)	8*d*	0.034(3)	0.096(2)	0.256(2)	1	0.84(12)
O(2)	4*c*	0.334(4)	1/4	0.687(2)	1	0.95(14)
O(3)	8*d*	0.101(7)	0.121(4)	0.537(4)	0.5	2.37(15)
O(4)	8*d*	0.33(1)	0.120(6)	0.494(5)	0.5	2.37
O(5)	4*c*	−0.01(1)	1/4	0.5627(8)	0.5	2.90(19)
O(6)	4*c*	0.42(1)	1/4	0.481(7)	0.5	2.90

Note. Parameters in brackets are from Rietveld refinement.

TABLE 4
Bond Lengths (Å), Angles (deg.), and Bond Valences for Pb_2BiPO_6[a, b]

Bi–O(1) × 2	2.34(2)	*0.51*	O(1)–Bi–O(1) × 2		78(1)		
Bi–O(1) × 2	2.35(2)	*0.50*	O(1)–Bi–O(1) × 2		73(1)		
Bi–O(6)	2.59(5)	*0.26*	O(1)–Bi–O(1) × 2		121(2)		
		2.28	O(6)–Bi–O(1) × 2		78(1)		
			O(6)–Bi–O(1) × 2		143(1)		
Pb–O(1)	2.24(3)	*0.71*	P–O(2)	1.51(3)	*1.34*	O(1)–O(1) × 2	2.97(4)
Pb–O(1)	2.39(3)	*0.47*	P–O(3) × 2	1.47(6)	*1.49*	O(1)–O(1) × 2	2.80(4)
Pb–O(2)	2.68(2)	*0.22*	P–O(6)	1.41(10)	*1.75*	O(1)–O(3)	3.19(5)
Pb–O(2)	2.98(2)	*0.10*			**6.07**	O(1)–O(6)	3.13(7)
Pb–O(3)	2.64(6)	*0.24*				O(2)–O(3)	2.50(5)
Pb–O(3)	2.84(6)	*0.14*				O(2)–O(6)	2.42(8)
Pb–O(6)	3.20(9)	*0.05*				O(3)–O(3)	2.34(7)
Pb–O(6)	3.24(5)	*0.05*				O(3)–O(3)	2.64(8)
		1.98				O(3)–O(6)	2.32(7)

[a] Oxygen contacts are listed for ≤ 3.2 Å.
[b] Bond valences are indicated in italic; valence bond sums are indicated in bold.

can also be considered to occupy the apex of a rectangular pyramid whose base is formed by the four O(1) atoms. Bi occupies alternate apexes on each side of the oxygen plane. The pyramids share O–O edges and thus form $(BiO_2)_\infty$ chains parallel to the *a* axis (Fig. 1). This oxygen coordination around Bi is common to many structures of the $M^{II}_2BiXO_6$ compounds (4) and is similar to the arrangement of the Bi_2O_2 sheets of the Aurivillius phases where a fifth oxygen, part of an octahedral layer, is bonded to Bi (18). A phase transition in (Sr, Ba)$Bi_2Ta_2O_9$ exists in which the Bi coordination changes from four to five at the Curie temperature (19).

The lead ions are coordinated to eight oxygen ions within a radius of about 3.2 Å (Table 4), forming a bisdisphenoid (Fig. 3). If the two O(6) are considered nonbonding then the polyhedron becomes a distorted octahedron. The lead atoms are located opposite the Bi atoms on the other side of the O(1) oxygen rectangular base and are bonded to two

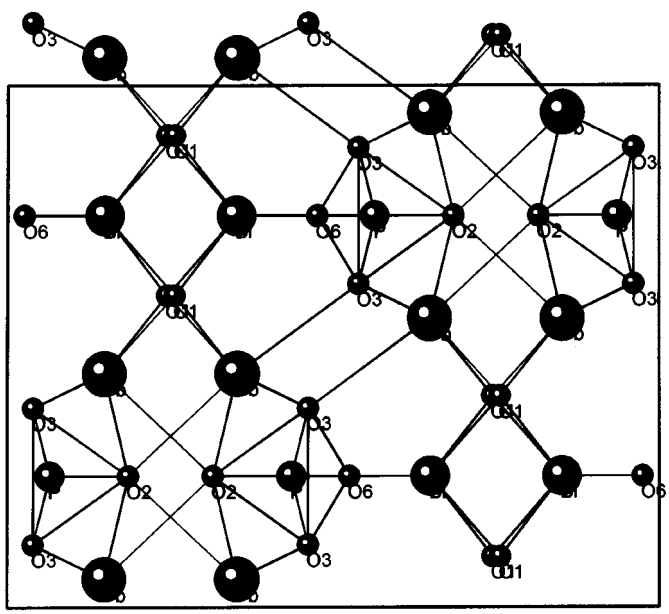

FIG. 1. The crystal structure of Pb_2BiPO_6. The view is down [100] and two *a* periodicities are drawn. The Pb–O6 bond is omitted for the sake of clarity. The origin is at the lower right corner.

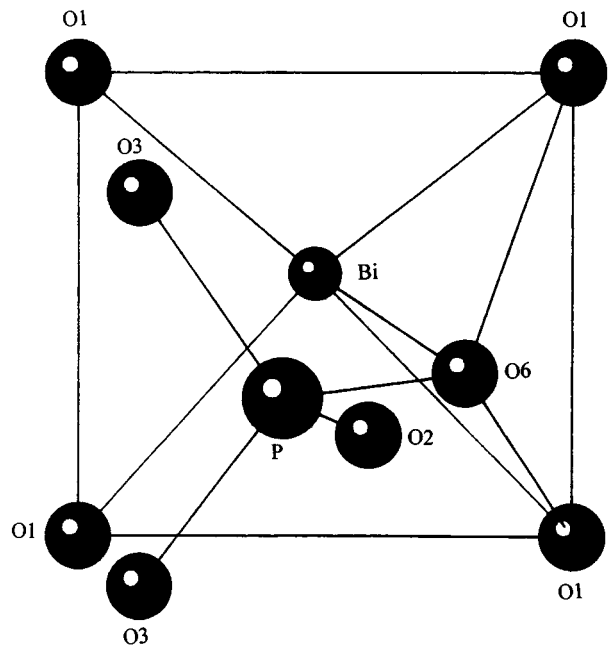

FIG. 2. The coordination polyhedron around Bi showing the linkage to one of the PO_4 groups.

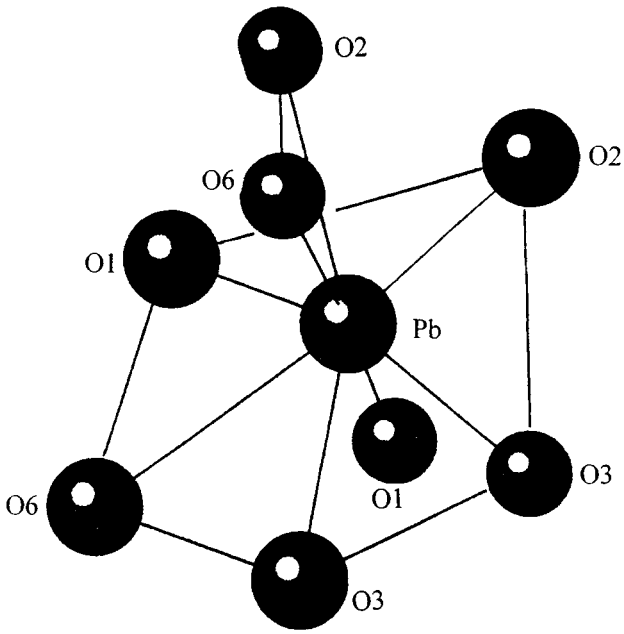

FIG. 3. View of the Pb coordination polyhedron to eight oxygen ions forming a bisdisphenoid.

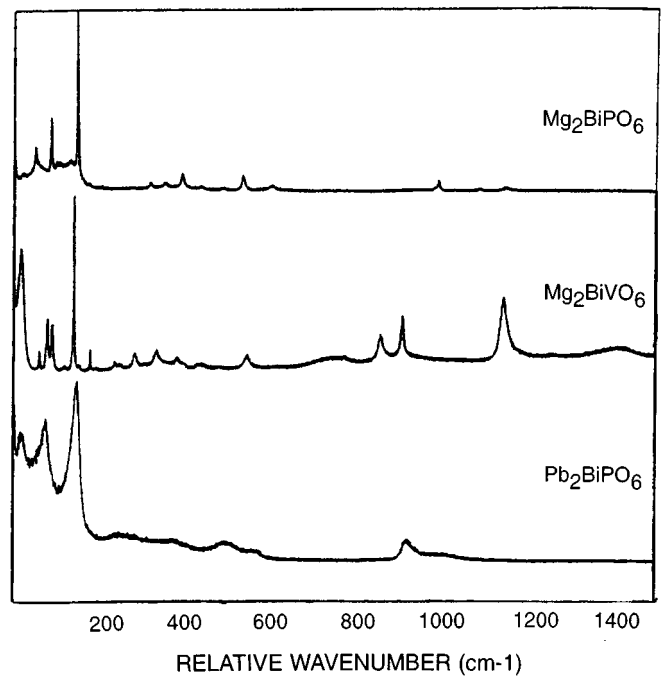

FIG. 4. Raman spectra of Pb_2BiPO_6, Mg_2BiVO_6, and Mg_2BiPO_6.

O(1) atoms. The coordination polyhedron is completed by O(3), O(2), and O(6) that are part of a face of a PO_4 tetrahedron, by O(6) and O(3) of another PO_4 group, and by O(2) of a third PO_4 group (Figs. 1 and 3). The Bi and Pb ions alternate parallel to the *a* axis (Fig. 1). The structure can also be described in terms of an irregular ($Bi_2O(1)Pb_2$) tetrahedron as found in Mg_2BiVO_6 (4). Two such tetrahedra share the Bi–Bi edge to form a dimer. The dimers build a chain parallel to the *a* axis, sharing a Pb–Bi edge. In both descriptions, with the $(BiO_2)_\infty$ chains or with (Bi_2OPb_2) tetrahedra, the phosphate is situated between two infinite chains bridging the Pb atoms and connecting to the Bi–O(1) layers through O(6).

The valence bond sum for Bi calculated on the basis of five bonding oxygen ions (Table 4) has the unexpected low value of 2.28 (20). In Mg_2BiVO_6 the four equal Bi–O bonds of 2.213(2) Å yield the valence bond sum 2.90, very close to the expected oxidation state 3+. The lengthening of the Bi–O(1) bonds to 2.34(2) Å in Pb_2BiPO_6 requires additional bonding to other anions for the usual 3+ oxidation state. With two additional anions at the same distance to complete a trigonal prismatic environment the valence bond sum would be 3. The valence bond sum for P calculated from the four bonding O^{-2} of Table 4 is 6.07. Evidently the usual oxidation states are established by the back-donation of almost a full electron from Bi to P. The empty *d* orbitals of fairly low energy on both P and Bi facilitate this process (21). The valence bond sum for Pb based on eight bonding O^{2-} has the expected value 1.96.

The crystal structures of Mg_2BiXO_6, X = V, P (4, 5), and Pb_2BiPO_6 are similar but are not isostructural and it is instructive to examine the Raman spectra of these three compounds (Fig. 4). The Raman bands for the Pb phase are broader, attributable to poorer crystallinity, and the statistical disorder of the phosphate group. The characteristic bands due to the XO_4^{3-} ion can be identified from the literature without ambiguity. The normal modes of vibrations for the isolated PO_4 moiety are $\nu_1(A_1) = 938\ cm^{-1}$, $\nu_2(E) = 420\ cm^{-1}$, $\nu_3(F_2) = 1017\ cm^{-1}$, $\nu_4(F_2) = 567\ cm^{-1}$ (22). For the isolated VO_4 ion the values are $\nu_1(A_1) = 826\ cm^{-1}$, $\nu_2(E) = 336\ cm^{-1}$, $\nu_3(F_2) = 804\ cm^{-1}$, and $\nu_4(F_2) = 336\ cm^{-1}$ (23). The frequencies of the vibrations for the tetrahedral ion in the three different phases are shown in Table 5. Two weak, broad bands are present in the range 500–550 cm^{-1}. These cannot be attributed to bridging V–O–V or P–O–P vibrations because one would expect those at higher frequencies, 650–800 cm^{-1}. They are due to

TABLE 5
Wave Numbers for Vibrations of the Tetrahedral Ion XO_4^{3-} ion in different compounds

Compound	Stretching ν_s and ν_{as}, cm^{-1}	Angular deformations δ_s and δ_{as}, cm^{-1}
Pb_2BiPO_6	946–924–1008	557–493–405–372
Mg_2BiPO_6	991–943	632–599–532–485–435–391
Mg_2BiVO_6	911–864–773	544–433–392–381–307–285

links in which V or P is involved and they are assigned to V/P–O–Pb and V/P–O–Bi. The reason for the lower frequencies is due to the involvement of the heavy metals. The intense bands between 143 and 150 cm^{-1} are present in every spectrum. These cannot be assigned to lattice vibration modes because the compounds crystallize in different systems. It is more likely an internal mode in which the heavy metals give rise to the low frequency vibrations. One can attribute these bands to internal modes of vibrations of the BiO_4 pyramid.

ACKNOWLEDGMENTS

We gratefully acknowledge Dr. Annick Lorriaux-Rubbens, Laboratoire de Spectochimie Infrarouge et Raman, Villeneuve d'Ascq, France for her indispensable assistance in the recording and interpretation of Raman spectra. H.S. acknowledges the support of this research by the R. A. Welch Foundation, Houston, Texas.

REFERENCES

1. A. I. Agranovskaya, *Izv. Akad. Nauk. SSSR, Ser. Fiz.* **24,** 1275 (1960).
2. L. G. Nikiforov, V. V. Ivanova, Yu. N. Venevtsev, and G. S. Zhdanov, *Inorg. Mat.* **4**(3)**,** 319 (1968).
3. L. G. Nikiforov, S. I. Urbanovich, and V. V. Shuvalov, *Russ. J. Inorg. Chem.* **55**(7)**,** 1065 (1981).
4. J. Huang and A. W. Sleight, *J. Solid State Chem.* **100,** 170 (1992).
5. J. Huang, Q. Gu, and A. W. Sleight, *J. Solid State Chem.* **105,** 599 (1993).
6. F. Abraham, M. Ketatni, G. Mairesse, and B. Mernari, *Eur. J. Solid State Inorg. Chem.* **31,** 313 (1994).
7. N. Tancret, S. Obbade, F. Abraham, F. Kzaiber, and B. Mernari, *J. Phys.* in press.
8. J. C. Boivin, Thèse d'Etat, Université des Sciences et Technologies de Lille, Lille, France, 1975.
9. M. F. Debreuille-Gresse, Thèse de Doctorat, Université des Sciences et Technologies de Lille, Lille, France, 1986.
10. S. Lazure, C. Vernochet, R. N. Vannier, G. Nowogrocki, and G. Mairesse, *Solid State Ionics* **90** (1–4), 117–123 (1996).
11. A. Mizrahi, J. P. Wignacourt, M. Drache, and P. Conflant, *J. Mater. Chem.* **5**(6)**,** 901 (1995).
12. P. E. Werner, L. Eriksson, and M. Westdahl, *J. Appl. Crystallogr.* **18,** 367 (1985).
13. J. Rodriguez-Carvajal, M. T. Fernandez-Diaz, and J. L. Martinez, *J. Phys. Condensed Matter* **3,** 3215 (1991).
14. J. De Meulenaer and H. Stompa, *Acta Crystallogr.* **19,** 1014 (1965).
15. G. M. Sheldrick, "SHELX76, Program for Crystal Structure Determination," University of Cambridge, England, 1976.
16. W. H. Bauer, *Acta Crystallogr. B* **30,** 1195 (1974).
17. D. W. J. Cruickshank, *Acta Crystallogr.* **17,** 677 (1964).
18. B. Aurivillius, *Arkiv Kemi.* **2,** 519 (1950).
19. R. E. Newnham, R. W. Wolfe, R. S. Horsey, F. A. Diaz-Colon, and M. I. Kay, *Mater. Res. Bull.* **8,** 1183 (1973).
20. I. D. Brown and D. Altermatt, *Acta Crystallogr. Sect. B* **41,** 244 (1985).
21. F. Albert Cotton and Geofffrey Wilkinson, "Advanced Inorganic Chemistry," 4th ed. p. 440. Wiley, New York, 1980.
22. E. Steger and K. Herzog, *Z. Anorg. Allgem.* **331,** 169 (1964)
23. K. Nakamoto, "Infrared and Raman Spectra of Inorganic and Coordination Compounds," 3rd ed. p. 142, Wiley–Interscience, New York, 1977.